64-2

Office of Naval Research

Contract Nonr-1866(32) NR-371-016

A STUDY OF CIRCULAR ARRAYS
-1-
EXPERIMENTAL EQUIPMENT

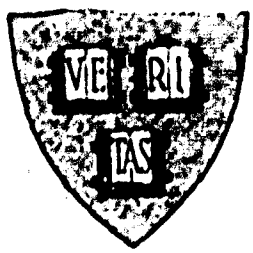

By

Richard B. Mack

May 1, 1963

Technical Report No. 381

Cruft Laboratory
Harvard University
Cambridge, Massachusetts

Office of Naval Research

Contract Nonr-1866(32)

NR - 371 - 016

A STUDY OF CIRCULAR ARRAYS

-1-

EXPERIMENTAL EQUIPMENT

by

Richard B. Mack

May 1, 1963

The research reported in this document was made possible through support extended Cruft Laboratory, Harvard University, jointly by the Navy Department (Office of Naval Research), the Signal Corps of the U. S. Army, and the U. S. Air Force, under ONR Contract Nonr-1866 (32). Reproduction in whole or in part is permitted for any purpose of the United States Government.

Technical Report No. 381

Cruft Laboratory

Harvard University

Cambridge, Massachusetts

PREFACE

This report is one of a series of six presenting the results of an experimental and theoretical investigation of circular arrays of antennas. The objects of the investigation were to demonstrate that circuit and radiation properties can be accurately predicted for arrays of physically real elements (as distinguished from the idealized elements usually assumed in conventional theory) over a wide range of element lengths, diameters, spacings, etc., to tabulate the useful results for small arrays; and for larger arrays, to reduce the theory to a relatively simple form for engineering applications.

All of the theoretical results were obtained from the quasi-zeroth-order theory recently worked out by King. The investigation shows that this theory will accurately predict driving point admittances and radiation patterns for real radiating elements which are less than about 1.2λ in length. In contrast, the commonly used zeroth order theory never gives the correct driving point admittances, and will accurately predict radiation patterns only when the elements are not longer than $\lambda/2$ and are in nearly identical electrical environments.

The general title of the report is "A Study of Circular Arrays". The six parts, which are issued as separate technical reports for convenience, are:

T.R. No. 381	"Experimental Equipment"
T.R. No. 382	"Self and Mutual Admittances"
T.R. No. 383	"Radiation Patterns and Current Distributions"
T.R. No. 384	"Tables of Quasi-Zeroth-Order $\psi_{dR}^{m}(h)$, $T^{m}(h)$, $T'^{m}(\lambda/4)$, Admittances, and Quasi-First-Order Susceptances"
T.R. No. 385	"Tables of E(h,s), C(h,s), S(h,s) For Circular Arrays of Up to Five Elements"
T.R. No. 386	"Plan for Practical Application to Arrays of Twenty or Fewer Elements"

TABLE OF CONTENTS

LIST OF FIGURES*

*Figures appear in numerical order following p. 1-R-2 (References).

LIST OF TABLES

ABSTRACT

Construction details are given for experimental equipment designed to permit measurement of the self and mutual admittances, current distributions along the radiating elements, and far field radiation patterns of small antenna arrays. The antennas are formed by extending the longitudinally slotted inner conductor of a rigid coaxial line beyond a large groundplane while terminating the outer conductor on the groundplane. A small balanced loop probe can be moved along the slot to sample the tangential magnetic field near the conductor. Measurement errors due to the probe are discussed. The array under test can be rotated by means of a turntable which is described. Radiation patterns are measured by transmitting with the array under test and receiving with a corner reflector antenna mounted on the groundplane but in the far field of the array. Although designed for 663 Mcps the equipment will operate over a wide range of frequencies.

ACKNOWLEDGMENTS

The author is particularly grateful to Professor Ronold W. P. King for his encouragement and help during this work, to Mr. Charles W. Sampson who built the equipment, to the Cambridge Research Laboratories which enabled the author to carry out the work by granting a leave-of-absence from his regular duties, and for the support extended to the project by Joint Services Research Contract Nonr 1866(32).

CHAPTER 1

EXPERIMENTAL EQUIPMENT

1.1 Introduction

The equipment to be described in the following sections was designed to permit measurement of self and mutual admittances, current distributions along the radiating elements, and far-field horizontal-plane radiation patterns. The design is based on somewhat similar equipment developed previously at Harvard [1,2,3] which, however, could not be used to measure radiation patterns. Basically, the apparatus consists of rigid coaxial lines with outer conductors terminated on a groundplane and longitudinally slotted inner conductors extending beyond the groundplane surface to form the radiating elements. These lines are mounted in a turntable which can be rotated through 360° to permit measurement of radiation patterns. The top of the turntable is a circular disk whose top surface fits flush with the free space surface of the groundplane through a circular opening in the groundplane. A corner reflector antenna is mounted on the groundplane sufficiently far from the circular disk to be in the far field of any arrays to be used. A small balanced-loop probe moving in the slotted inner conductor of the coaxial line can be used to measure the relative tangential magnetic field in the vicinity of the conductor and hence the surface current along the conductor. From a knowledge of this current distribution along the coaxial line, the apparent admittances terminating the line can be found. When the probe is moved along that part of the inner conductor which is

extended beyond the groundplane the relative current distributions along the radiating elements are obtained. This experimental model has been extensively analyzed by King [4] and correlated with the usual theoretical model of thin dipoles center driven by a discontinuity in scalar potential.

Although the equipment will operate over a wide range of frequencies, it was specifically built for 600 to 800 Mcps. This choice represents a compromise of several opposing factors. As the frequency is increased, coaxial line terminal-zone effects [5] become more important, maximum probe sizes decrease, critical machining tolerances decrease, reflections from groundplane irregularities become more important, and the uncertainty in distance measurements becomes a significant part of a wavelength. As the frequency is decreased, the required coaxial lines and groundplane size become larger for a given measuring accuracy and the antenna length beyond the groundplane becomes longer making it more difficult to hold straight.

If the approximate range of terminating admittances to be measured is known, the characteristic admittance of the measuring line should be chosen to give standing waves convenient for the measuring procedure to be used. However, this consideration must be tempered by several additional requirements. The probe actuating rod must maintain a good sliding contact with the inner surface of the brass tube used as coaxial line inner conductor and antenna. Only a few such tubing combinations are available and this determined the antenna diameter of 0.2500" . An outer conductor must now be used whose inner diameter is sufficiently

large to contain the probe and whatever material is used to support the inner conductor. The inner diameter of the outer conductor should also be as small as possible to reduce the end effects. A compromise of these requirements led to an outer conductor with an inner diameter of 0.7500", so that the ratio of the inner diameter of the outer conductor to the outer diameter of the inner conductor, b/a, was 3.

In order to provide identical antennas for a five element array, five of the measuring line and antenna assemblies described in Sections 1.2 and 1.3 were constructed. These were made mechanically alike within the machining tolerances.

1.2 Measuring Line and Antennas - Mechanical Characteristics

Assembly and construction details of the measuring line and antennas are shown in Figs. 1-1 - 1-6. The important features of the coaxial measuring line is a longitudinally slotted inner conductor which can be extended precisely measured amounts beyond the outer conductor by means of the Antenna Adjustor Carriage (Figs. 1-1, 1-3, 1-6(f)) and a small Enhanced Loop Probe (Figs. 1-5, 1-7(b)) which can be moved along the slotted inner conductor by means of the Probe Actuating Rod (Fig. 1-1) and Probe Adjustor Carriage (Figs. 1-1, 1-3, 1-6(f)). Power picked up by this probe is transmitted to a Type N connector on the Probe Adjustor Carriage (Fig. 1-1) by means of a coaxial line formed by replacing the outer conductor of RG-58/U coaxial cable with the Probe Actuating Rod.

Power is fed to the measuring line through a Feeding Stub (Figs. 1-1, 1-2, 1-6(a)) whose inner conductor makes a sliding contact with

the 0.2500" diameter inner conductor of the measuring line. The bottom end of the measuring line is closed by means of a short-circuiting end cap (Fig. 1-1, 1-6(a)) which makes a tight sliding fit with the inner conductor. To maintain the inner conductor concentric with the outer conductor, HD-2 Styrofoam is used to fill the space between inner and outer conductors. This Styrofoam is turned to make a tight fit with the outer conductor, a good sliding fit with the inner conductor, and has a slot milled for the probe (Fig. 1-6(c)).

The coaxial line is attached to a 7/8" square brass supporting tube (Fig. 1-1) through two Line Support Brackets (Fig. 1-1). These Line Support Brackets are split so that the outer conductor can be retracted to permit installation of the coaxial line assembly in the Turntable (Fig. 1-7). The supporting tube also contains a rack along which the Probe Position Adjustor and Antenna Length Adjustor can be moved. Verniers are attached to the carriages and a centimeter scale is attached to the supporting bracket. The entire assembly is attached to the underside of the circular disk which forms the turntable top (Fig. 1-9(a)) by the Top Mounting Flange (Figs. 1-1, 1-6(b)) so that the end of the outer conductor is flush with the top of the groundplane. The assembly is attached to the Turntable Bottom Plate (Figs. 1-8, 1-9(b)) by inserting the Bottom Support (Fig. 1-1) in the appropriate hole of the turntable bottom plate.

Certain measurements require the antennas to be short-circuited at their driving point or at some other known point. The short circuit must maintain good electrical contact between the inner and outer conductors and not extend significantly above the groundplane surface. A small extension above the groundplane made a shoulder possible

which served to positively position the short-circuiting plugs with respect to the groundplane surface and had no detectable effect on the measurements.

To accommodate a 0.1250" extension of the short-circuiting plugs into the coaxial line, the Styrofoam filling ended inside of the line and thin Styrofoam disks were used to extend the filling to the line end when shorting plugs were not required.

When using this short-circuiting plug as a reference for impedance or admittance measurements, a correction must be made, since the reference plane is inside the coaxial line instead of at the surface of the groundplane. For the admittance measurements discussed in Chapter 2, two different short-circuiting plugs were used. One of these extended 0.3175 cm and the other 0.2540 cm into the coaxial line.

Construction details of the Balanced Loop Current Probe are given in Fig. 1-5. It is made of a special 50 ohm cable obtained from the Precision Tube Company of Philadelphia. The inner conductor is 0.013" in diameter, the dielectric is fiberglass, and the outer conductor has an inner diameter of 0.031" and outer diameter of 0.039". The probe area was approximately 2.24×10^{-6} square wavelengths at 663 Mcps. This was chosen as the largest probe which gave no evidence of absorbing excessive amounts of power from the transmission line. Actually, two larger probes with areas of about 58×10^{-6} and 19.6×10^{-6} square wavelengths gave evidence of broadening the current maximum on a short-circuited line.

Measurement errors which result from mechanical irregularities in slotted lines are discussed by Ginzton [6]. Two aspects are particularly

important for the equipment being discussed here. The slot in the inner conductor must be of uniform width over its entire length and the probe holder must make a good sliding fit both with this slot and the inner conductor. If distances between the inner and outer conductors are maintained by filling the line with short sections of Styrofoam, as was done in the lines being described here, the Styrofoam must be carefully turned to size and so fitted into the line that the milled probe slots in successive sections are properly aligned. The lines were each tested by using the short-circuiting plugs at the groundplane surface and measuring the current distribution along the entire line.

1.3 Measuring Line and Antennas - Electrical Characteristics

HD-2 Styrofoam made by Dow Chemical Company was used to fill the region between the inner and outer conductors. This material is described by Dow [7] as having a relative dielectric constant of approximately 1.07 and a loss tangent of less than 4×10^{-4}. Repeated measurements of λo, the wavelength in air, and λg, the wavelength in the line, gave

$$\frac{\lambda o}{\lambda g} = \sqrt{\epsilon_r} = 1.0289 \qquad \epsilon_r = 1.0586 \quad \text{(experimental)}$$

This is the value used in the following calculations. The conductivity of brass was chosen as $\sigma_{Brass} = 1.200 \times 10^6$ mhos/meter [8]. This is only an approximate value, since the actual value will vary considerably

with different lots of brass. 663 Mcps was chosen as the operating frequency. The various parameters are [9]

$$\omega = 2\pi f = 4.166 \times 10^{9} \text{ rad/sec.}$$

loss t[illegible] $h_s = \frac{\zeta}{\zeta_T}$; $\sigma_{HD-2} < 1\ 578 \times 10^{-5}$ mhos/meter

inner radius of outer conductor $b = 3/8" = 9.525(10^{-3})$ meters

outer radius of inner conductor $a = 1/8" = 3.175(10^{-3})$ meters

$$b/a = 3$$

shunt conductance $g = \frac{2\pi\sigma_{HD-2}}{\ln\ b/a} < 9.025 \times 10^{-5}$ mhos/meter

shunt capacitance $c = \frac{2\pi\ \epsilon_0\epsilon_r}{\ln\ b/a} = 53.58 \times 10^{-12}$ farads/meter

series resistance $r = \frac{1}{2\pi}\left(\frac{1}{a} + \frac{1}{b}\right)\sqrt{\frac{\mu\omega}{2\sigma}}_{Brass} = .9874$ ohms/meter

external series inductance $\ell^e = \frac{\mu}{2\pi} \ln b/a = 2.197(10^{-7})$ henrys/meter

distortion factor $\phi_c = \frac{1}{2\omega}\left[\frac{r}{\ell} - \frac{g}{c}\right] \sim 3 \times 10^{-4}$

conditions for low loss line

$$\left(\frac{r}{\omega\ell}\right)^2 << 1 \quad , \quad \left(\frac{g}{\omega c}\right)^2 << 1 \quad , \quad \frac{rg}{\omega^2 \ell c} << 1$$

$$\frac{r}{\omega\ell} = .1079(10^{-2}), \quad \frac{g}{\omega c} = .0404(10^{-2}), \quad \frac{rg}{\omega^2 \ell c} = .362(10^{-7})$$

characteristic impedance $R_c = \sqrt{\frac{\ell^e}{c}} = 64.1$ ohms

R_c will be slightly changed by the 1/16" slot in the inner conductor. The effect of the slot may be computed from [10]

$$\frac{\Delta R_c}{R_c} = \frac{1}{4\pi^2} \frac{\omega^2}{b^2 - a^2} \simeq 8 \times 10^{-4}$$

where ω is the slot width.

attenuation $\alpha = \frac{\sqrt{\ell^e c}}{2} \left[\frac{r}{\ell} + \frac{g}{c}\right] = 1.060 \times 10^{-2}$ nepers/meter

propagation constant $\beta = \omega\sqrt{\ell^e c} = 14.29$ rad/meter

phase and group velocity $v_p = v_g = \frac{1}{\sqrt{\ell^e c}} = 2.914 \times 10^8$ meters/second.

Summary:

$R_c = 64.1$ ohms	$v_p = v_g = 2.914 \times 10^8$ meters/sec.
$\alpha = 1.060 \times 10^{-2}$ nepers/meter	$c = 53.58$ μμf/m.
$\beta = 14.29$ rad/meter	$\ell^e = .2197$ μh/m.
$\phi_c = 3 \times 10^{-4}$	$r = .9874$ Ω/m.

1.4 Turntable Mount

Arrays of the antenna and measuring line assemblies were mounted in a Turntable Mount (Figs. 1-7, 1-8) which attached them to the ground-plane and provided a means of rotating the arrays for pattern measurements. The turntable consists of a Top Disk (Figs. 1-7, 1-8(a)) , a Bottom Plate (Figs. 1-7, 1-8(b)) , a bottom yoke and bearing, and two

connecting rods (Fig. 1-7) . The top carried most of the weight and was supported on six Bearing Supports (Fig. 1-7) . These bearings were adjusted to maintain a good sliding contact between the top disk and the groundplane. Locking screws in the bearing supports could be used to raise the top disk slightly above the roller bearings and lock it against the groundplane. For each desired antenna location, appropriate holes in the top disk were bored and reamed to 0.8125" to make a good fit with the coaxial line outer conductor. To permit a large number of holes near the disk center, a 16.662" section in the disk center was replaceable. Plugs (Fig. 1-7) were made to fill the antenna position holes not being used.

The bottom plate (Figs. 1-7, 1-8(b)) was cut from 0.1250" aluminum sheet and mounted on a supporting frame made from 0.6250" aluminum bars. Holes to support the bottom end of the measuring line were laid out with the same center locations as for the top disk but were drilled and reamed to 0.3125" . Additional disks centered and bolted on top of the bottom plate were used to prevent the required holes from overlapping. A circular scale with $\frac{1}{2}^{\circ}$ divisions was mounted on the bottom plate supports. This, together with a reference pointer attached to the floor, gave the angular position required for radiation patterns.

All circular arrays were designed to have the antennas equally spaced about a circle so that the antennas were actually located at the apexes of equilateral polygons of side d . Insert plates (Fig. 1-8) with a wide range of spacings were used for arrays of N = 3, 4, 5 elements . A single plate was used for N = 2 . A listing of the spacings provided is given in Tables 1-1 and 1-2 . For a circular array of N elements

located at apexes of equilateral polygons, d is the side of the polygon and S is the radius of a circle passing through the apexes so that

$$S = \frac{d}{2 \sin \pi/N} .$$

For a linear array, d is used to represent simply the center-to-center distance between the elements.

TABLE 1-1

CIRCULAR ARRAY SPACINGS
λo = 17.800 "

	S(inches)		
d/λ	N=3	N=4	N=5
0.1250	1.285	1.574	1.894
0.1875	1.928	2.361	2.838
0.2500	2.569	3.148	3.785
0.3125	3.213	3.935	4.730
0.3350		4.217	
0.3400			5.148
0.3600			5.451
0.3750	3.854	4.721	5.679
0.4000		5.035	
0.4100	4.213		
0.4250		5.349	
0.4375	4.498	5.509	6.622
0.4650	4.779		
0.4750		5.979	7.274
0.5000	5.138	6.293	7.571
0.5150		6.482	
0.5300	5.447		
0.5400		6.797	
0.5625	5.783	7.083	
0.5850	6.012		
0.6250	6.423		9.464*
0.6875	7.068		
0.7250	7.451		
0.7500		9.440*	11.353*
0.8750	8.993*	11.014*	13.245*
1.0000	10.278*	12.587*	

TABLE 1-2

LINEAR ARRAY SPACINGS

d/λ	d (inches, λ=17.800")
.0625	1.115
.1000	1.780
.5000	7.125 at f = 828.5 Mcps.

* indicates holes are located on main disk. Other holes are on insert plates.

1.5 Groundplane

A 24' x 48' rectangular groundplane was available for the experiment. Its surface consisted of 0.1250" aluminum plates fastened by stainless steel flat-head screws to a supporting structure of 3" aluminum channels and 6" I beams. The surface plates were all 4' wide but had lengths of 12', 8', and 4' and were arranged so that the seams between the plates were staggered to reduce reflections. Fig. 1-9 shows the arrangement of the surface plates, the corner reflector antenna, and the circular disk. All arrays to be used in the experiment were confined to the area of the circular disk and this was mounted so as to be different distances from all four edges of the groundplane. The closest edge was about 6.75 λ from the disk center. An array of one driven and two parasitic antennas, the top surface of the circular disk, and the adjacent groundplane are shown in Fig. 1-10.

1.6 Groundplane $\vec{E}$ Probe

A simple method of adjusting two antennas to have equal amplitude but opposite phase is to place a charge probe midway between the antennas and adjust the phase and amplitude of one until no power is received on the charge probe. The probe used for such measurements with this equipment is shown in Fig. 1-6(g). It was made by drilling a 0.2500" hole in an antenna position hole plug, attaching a Type N chassis connector to the plug, soldering a wire to extend the inner conductor, and adding a Teflon bushing to fill the space between the cover and inner conductor. When placed midway between the antennas, this probe

provided sufficient sensitivity so that a null could be obtained which was 40-45 db below the inphase maximum condition.

1.7 Corner Reflector Antenna

Dimensions of the corner reflector were based on the experimental work of Harris [11], and details of the actual antenna used are shown in Fig. 1-11. The reflector sides were approximately $\lambda/2$ high and 2λ long and the associated monopole was $\lambda/4$ long. The reflector was fastened to the groundplane by 1" aluminum angles. Several folds of aluminum foil were placed between the angle brackets and groundplane to insure good contact. A distance of $0.975\,\lambda$ (17-3/8") between the monopole and reflector corner was found experimentally to produce best results. For this monopole-to-reflector distance the gain was about 12 db above that of the monopole with no reflector. The radiation patterns could not be measured, but some estimate of the main beam shape could be obtained by rotating the reflector about the monopole while transmitting from the measuring line and antenna located on the circular disk. In this way, the beam was found to be about 40 degrees wide and to have no side lobes higher than 11-12 db below the beam maximum.

1.8 Transmitting and Receiving Equipment

Simplicity, operational reliability, and equipment availability were foremost considerations which led to an amplitude modulated transmitting and receiving system shown in Fig. 1-12. Aprroximately 250 milliwatts of power at 663 Mcps was provided by a General Radio Type 1209-B

unit oscillator. This was approximately 30% modulated by a General Radio Type 1214-A Unit Audio Oscillator operating at 1000 cps. A 3 or 6 db attenuator was used to pad the oscillator so that the net power available for the experiment was 50-100 milliwatts. For most measurements this gave an operating range of 25-35 db above the receiver noise level. The only difficulties caused by this limited sensitivity were experienced in measuring the current distributions on parasitic elements when $\beta h = \pi, \frac{5\pi}{4}$. For these measurements ten to twenty db greater sensitivity would have been desirable.

IN21 crystals and holders used for detection were matched to a VSWR of 1.05 or less over the range of incident power used. Signals from the crystals were amplified by Electronic Corporation of American Type TA A-16 EA bolometer amplifiers and fed to Ballantine Type 300 or Type 300D voltmeters. Several of these combinations were used at different points in the equipment. Only those units actually used for measurements were calibrated.

The matching units consisted of either Microlab Model S2-05N double stub tuners or a combination of General Radio Type 874-LK line stretchers and sliding short circuits. Considerable vibration problems were encountered with all of the equipment and it was finally mounted with foam rubber pads on 0.7500" plywood sheets which were fastened to a brick wall. The amplifiers were placed on foam rubber pads in a sturdy metal rack which also was fastened to the brick wall. The mounting arrangement is shown in Fig. 1-13.

The phase of an unknown signal could be measured by differencing the unknown signal and a reference signal from the directional coupler (Fig. 1-12) . A coaxial hybrid tee and matched detector served as the differencing device. The electrical path length of the reference signal could be varied by means of a phase line, which was a rigid coaxial line terminated in its characteristic admittance, but otherwise very similar to the lines described in Sections 1.2 and 1.3 . A reference signal from the directional coupler was introduced into the phase line through a side arm feeding stub and extracted through a probe which could be moved along the slotted inner conductor. On a flat line (VSWR = 1.000) the electrical path length through the phase line is directly proportional to the distance from the feeding stub to the probe. When adjusted for best match, the phase line still had a VSWR $\approx$ 1.05 .

With this system, relative phases are measured by introducing both the unknown and reference signals into a hybrid tee and adjusting the path length of the reference signal by known amounts until a null is indicated by the detector. A sharp null is obtained only if the unknown signal and the reference signal have very nearly equal amplitudes. For the measurement of phase along an antenna which has wide amplitude variations, this requires frequent amplitude adjustments to the reference signal with their associated phase corrections.

Two improvements which were not available at the time of this experiment can considerably increase the ease and accuracy of phase measurements. The first of these, discussed by Whiteside [12], consists of replacing the phase line by a General Radio Type 874-LT constant

impedance trombone line stretcher. When mounted on a firm base and fitted with a rack, pinion, scale, and vernier this type of line stretcher makes an excellent constant-amplitude -UHF-phase shifter which is not only much smaller physically than the phase lines described above, but which also introduces essentially no standing wave. The second, discussed by King [13] and by Burton [14], involves the use of a balanced detector instead of a single detector at the output from the hybrid junction. This system provides a deep null which is independent of the relative amplitudes of the unknown and reference signals.

1.9 Detector Calibration

The crystal, amplifier, and meter were calibrated as a unit by using the region about a current maximum on a short-circuited measuring line described in Sections 1.2 and 1.3. If a transmission line is terminated in a reasonably good short or open circuit, the current distribution near the maximum follows a cosine law. The calibration procedure was to set the amplifier gain to a convenient level, adjust the power to the desired starting level, and to then measure the half-power curve widths for a number of different power levels. The response law, n , is given by [15]

$$n = \frac{\log 1/2}{\log \cos \left(\frac{\pi L}{\lambda_g}\right)} \qquad (1.1)$$

where L = distance between half-power points,

λ_g = wavelength on measuring line.

Results from such measurements are given in Table 1-3 and indicate an average response law of $n = 2.04 \pm .02$ for meter readings between .01 and 6.30 volts, or a useful range of about 30-35 db. For several power levels the entire distribution curve in the vicinity of the maximum was read, graphed, and the half power points determined from the graph. The values of n from this data ranged from 1.99 to 2.01. Thus the response was assumed to be square law over the useful range of meter readings. Periodic checks during the experiment indicated no substantial change from square law.

When the calibration is done on a carefully constructed slotted line using a probe which does not load the line, the principal error in n comes from uncertainty in locating the half-power points. Each half-power point for which the distribution curve was not plotted could be found to about $\pm .02$ cm corresponding to a total uncertainty in L of $\pm .04$ cm. The effect on n of this uncertainty in L may be found by forming the derivative of equation (1.1).

$$\frac{\Delta n}{n} = \log_{10} e \left[\frac{\frac{\pi L}{\lambda_g} \tan \frac{\pi L}{\lambda_g}}{\log_{10} \cos \frac{\pi L}{\lambda_g}} \right] \tag{1.2}$$

assuming a response law near 2, $\frac{\pi L}{\lambda_g} \approx \frac{\pi}{4}$, and $\lambda_g = 43.90$ cm

$$\frac{\Delta n}{n} = 2.874 \frac{\pi \Delta L}{\lambda} = .00822 \tag{1.3}$$

This corresponds to the most probable error of $\pm .02$ computed from the values on n in Table 1-3.

TABLE 1-3

DETECTOR CALIBRATION
$\lambda_g/2 = 21.935$ cm

Output meter reading (volts)	Location of Half Power Points		L (cm)	n
	1st (cm)	2nd (cm)		
24.3	35.10	22.93	12.17	1.573
19.8	34.85	23.16	11.69	1.728
15.8	34.65	23.335	11.315	1.860
12.3	34.55	23.435	11.115	1.938
9.80	34.60	23.45	11.15	1.925
7.93	34.545	23.48	11.065	1.960
6.30	34.46	23.59	10.87	2.041
5.03	34.46	23.58	10.88	2.038
4.00	34.425	23.57	10.885	2.052
3.12	34.39	23.57	10.82	2.064
2.51	34.46	23.55	10.91	2.025
2.00	34.42	23.59	10.83	2.060
0.98	34.46	23.59	10.87	2.041
0.79	34.465	23.55	10.915	2.024
0.78	34.50	23.525	10.975	1.999
.620	34.47	23.59	10.88	2.038
.495	34.50	23.55	10.95	2.008
.396	34.44	23.61	10.83	2.060
.396	34.42	23.63	10.79	2.077
.320	34.46	23.61	10.85	2.051
.250	34.50	23.60	10.90	2.030
.198	34.47	23.60	10.87	2.041
.155	34.43	23.62	10.81	2.068
.123	34.43	23.61	10.82	2.064
.100	34.46	23.60	10.86	2.040
.0790	34.49	23.57	10.92	2.022
.0790	34.50	23.58	10.90	2.030
.0630	34.45	23.60	10.85	2.051
.0500	34.49	23.60	10.89	2.034
.0390	34.46	23.61	10.85	2.051
.0313	34.47	23.59	10.88	2.038
.0200	34.50	23.57	10.93	2.017
.0200	34.50	23.58	10.92	2.022

Average $n = 2.04$ between .01 and 6.30 volts

Most probable error $\Delta n = \pm .02$

1.10 Tests for Spurious Groundplane Reflections

Several potential sources of error in the measurements are contained in the groundplane arrangement of Fig. 1-10. Reflections from the edges of the groundplane, reflections from seams between the surface plates, and erratic electrical contacts between the circular disk and the groundplane may all contribute irregularities to the measured radiation patterns and admittances. Except near the driving points, the current distributions will not be seriously affected by small changes in currents along the groundplane. The actual reflection coefficients of the groundplane edges were not measured but several attempts were made to find irregularities in the measurements which might be caused by such reflections.

When the antenna radiation pattern has a deep null pointed toward the corner-reflector receiving antenna (Fig. 1-9), the beam maximum may be pointing toward the reflector edge at a correct angle so that energy from the edge is reflected toward the receiving antenna. An attempt to find such interference is shown in Fig. 1-14 which is the measured and theoretical pattern for a two-element array fed with equal amplitude but opposite phase. There is no evidence of interference over the 25 db range of measurement.

A square groundplane as large as 6λ on a side has been shown by Meier and Summers [16] to produce serious errors in the measured reactances of single antennas with h/λ both near $1/4$ and $1/2$. The larger rectangular groundplane with the antennas mounted off center as used here may be expected to have much less effect on the admittances, and its effects should be a function of the array orientation with respect

to the various groundplane edges. Table 1-4 contains the results of admittance measurements on a three-element array for several values of h/λ and array orientations. Variations in the results are all within the expected uncertainties in measurement discussed in Chapter 2 and indicate no detectable effects from the finite size of the groundplane.

With a single transmitting antenna of length $h = \lambda/4$ located at the end of the row of position holes for linear arrays (Fig. 1-8(a)), the vertical component of the electric field, E_z, was measured across the disks in steps of $\lambda/16$ by inserting the groundplane $\vec{E}$ probe (Section 1.6) in the appropriate holes. In the north-south orientation the line of measurement was parallel to the long side of the groundplane and in the east-west orientation parallel to the short side of the groundplane. The results in Fig. 1-15 are normalized to $\rho = \lambda/4$ and agree with the expected theoretical variation for $\rho > .1875\lambda$. Again no disturbances from spurious reflections are indicated. For a sinusoidal current distribution [17]

$$E_z = \frac{-j\,Im\,\zeta_o}{4\pi}\left[\frac{e^{-j\beta R_{1h}}}{R_{1h}} + \frac{e^{-j\beta R_{2h}}}{R_{2h}} \frac{-2\cos\beta h}{R_o} e^{-j\beta R_o}\right] \qquad (1.4)$$

$$R_{1h} = \sqrt{(z+h)^2+\rho^2}\ , \quad R_{2h} = \sqrt{(z-h)^2+\rho^2}\ , \quad R_o = \sqrt{z^2+\rho^2}$$

Let $z = 0$, $\beta h = \pi/2$.

Then

$$|E_z| = \frac{\zeta_o}{2\pi} \frac{1}{\rho\sqrt{1+(h/\rho)^2}} \qquad (1.5)$$

and

$$P = 20\log\frac{|E_z|_\rho}{|E_z|_{\lambda/4}} = K\,\frac{1}{\rho\sqrt{1+(h/\rho)^2}} \qquad (1.6)$$

TABLE 1-4

ADMITTANCES FOR DIFFERENT ARRAY ORIENTATIONS

N = 3 , d/λ = 0.5000

h/λ	Conditions	Driving Voltages	ρ	ϕ'	Y_{SA} Re	Y_{SA} Im	Y_{11} Re	Y_{11} Im	Y_{12} Re	Y_{12} Im
0.6250	Disk Locked	B	0.151	-1.094	1.48	4.19	1.48	4.19	-0.13	-0.74
		C	0.151	-1.019	1.61	4.94				
0.6250	Disk Unlocked Beam is NW,SE	B	0.153	-1.094	1.50	4.19	1.50	4.19	-0.10	-0.73
		C	0.151	-1.020	1.60	4.92				
0.6250	Beam is NE,SW	B	0.152	-1.095	1.48	4.19	1.48	4.19	-0.10	-0.71
		C	0.149	-1.023	1.57	4.90				
0.6250	Beam is E,W	B	0.152	-1.096	1.48	4.17	1.48	4.17	-0.11	-0.74
		C	0.151	-1.021	1.60	4.92				
0.6250	Beam is SW,NE	B	0.152	-1.095	1.48	4.18	1.48	4.18	-0.14	-0.73
		C	0.153	-1.020	1.62	4.92				
0.2500	Beam is NW-SE	B	1.126	0.022	9.63	0.19	9.63	0.19	3.65	3.35
		C	0.647	0.905	5.98	-3.16				
0.2500	Beam is NE-SW	B	1.117	0.019	9.67	0.20	9.67	0.20	3.68	3.39
		C	0.644	0.903	5.98	-3.18				
0.2500	Beam is E-W	B	1.126	0.027	9.63	0.17	9.63	0.17	3.64	3.38
		C	0.642	0.900	5.99	-3.21				
0.2500	Beam is SW-NE	B	1.128	0.023	9.62	0.19	9.62	0.19	3.65	3.36
		C	0.645	0.906	5.97	-3.16				

1.11 Tests for Probe Loading and Sensitivity to Dipole Modes

When a probe extracts sufficient power from the transmission line to produce measurable changes in the distribution along the transmission line, the probe is said to load the line. The usual effect of probe loading is to make the observed maxima and minima appear displaced by different amounts from their true location and to make the observed maxima appear lower and broader than the true maxima [18,19]. On a short-circuited line there will be no shift of the minima but the shift of the maxima and broadening should be greatest. Fig. 1-16 shows the current maxima on a short-circuited line measured with the balanced loop probe described in Section 1.2. The theoretical curve is computed from

$$P = 20 \log |I| = 20 \log \cos 2\pi \ell/\lambda_g \qquad (1.7)$$

where ℓ is the distance along the line from the maxima and λ_g is the wavelength on the line. A 610 A bolometer and Hewlett Packard Model 415B standing wave indicator was used as detector to insure a true square law response. In Fig. 1-16 the experimental values agree to within 0.2 db with the theoretical values. There is a very slight indication of asymmetry about the maxima but this will be negligible with any admittances of interest terminating the line. The probe described in Section 1.2 was actually the smallest of three probes which were tried. The two larger probes seriously loaded the line, creating broadened and asymmetric maxima.

A detailed discussion of probe properties is given by Whiteside [12]. His general conclusion is that a center-loaded circular loop which is carefully made and which has a diameter less than $0.01\,\lambda_g$ will neither seriously load a transmission line nor have an undue sensitivity to the electric field. The probes described in Section 1.2 have a diameter of $0.0047\,\lambda_g$ and so come well within the "small probe" requirements at the measurement wavelength of $\lambda_g = 43$ cm .

If a center-loaded loop is to be used as a probe to measure the current distribution along a cylindrical conductor, currents maintained in the probe by the electric field must be negligible compared to those maintained by the magnetic field. Consider the usual cylindrical coordinate system ρ , θ , z , with the antenna and coaxial line concentric with the vertical z axis. Let the groundplane surface lie in the $z = 0$ plane, the coaxial line extend along the negative z axis, and the outer conductor be terminated at the groundplane surface. Inside the coaxial line away from the ends, the only fields are [20]

$$B_\theta = \frac{I_z(w)}{2\pi v_o \rho} = \frac{I_s}{2\pi v_o \rho (1-\Gamma_s)} \left(e^{\gamma w} - \Gamma_s e^{-\gamma w}\right) \tag{1.8}$$

$$E_\rho = \frac{I_s}{2\pi \epsilon v \rho (1 - \Gamma_s)} \left(e^{\gamma w} + \Gamma_s e^{-\gamma w}\right) \tag{1.9}$$

where I_s = current in transmission line load

Γ_s = reflection coefficient of load

$\gamma = \alpha + j\beta$ = propagation constant along the transmission line

w = distance to the load

ϵ = absolute dielectric constant of material filling the coaxial line

v = phase velocity in the coaxial line .

Currents maintained in opposite directions on opposite sides of the probe are said to be in the transmission-line mode and those in the same directions on opposite sides of the probe are said to be in the dipole mode [21]. B_θ maintains a transmission-line mode circulating current in the probe. E_ρ which is tangent to the horizontal sider of the probe maintains currents in these sides. If the w-variation in E_ρ is essentially constant over the probe diameters, and if the probe gap is perfectly symmetrically located, the currents due to E_ρ will charge both sides of the gap equally and therefore cause no net circulating current in the probe. Only near the voltage minimum on lines with very high standing wave ratios will E_ρ vary sufficiently rapidly with w to cause trouble. In this region, however, B_θ will be near a maximum and E_ρ near a minimum so that probe currents due to E_ρ will be negligible compared to those due to B_θ .

Since the probes are mechanically difficult to construct, each should be tested experimentally for symmetry. This can be done through two measurements on a short-circuited line. For a lossless line and a perfect short circuit

$$\alpha = 0 \quad , \quad \Gamma_s = -1$$

$$B_\theta = \frac{I_s}{2\pi \nu_o \rho} \cos \beta w \tag{1.10}$$

$$E_\rho = \frac{jI_s}{2\pi \epsilon \rho} \cos \beta(w+\lambda/4) = \frac{jI_s}{2\pi \epsilon \rho} \sin \beta w \tag{1.11}$$

The probe current is then (Ref. [12], equation VII-10b)

$$I_L(w) = S_B \cos \beta w + jS_E \cos \beta(w + \lambda/4) \qquad (1.12)$$

$$= S_B[\cos \beta w + j\epsilon \cos \beta(w + \lambda/4)] \qquad (1.13)$$

where S_B and S_E are sensitivity constants depending on the mechanical configuration of the probe and ϵ is an error ratio defined by $\epsilon = S_E/S_B$. In the method suggested by Whiteside, the relative probe current is measured with the probe located first at $w_o = \lambda/4$ (B_θ min) and then with the probe located at $w_1 = \lambda/2$ (B_θ max). Then

$$\frac{I_L(w_o)}{I_L(w_1)} = \frac{jS_E}{S_B} - j\epsilon \quad \text{or} \quad 20 \log\left|\frac{I_L(w_o)}{I_L(w_1)}\right| = 20 \log\left|\frac{S_E}{S_B}\right| = 20 \log|\epsilon| = \epsilon_{db} \qquad (1.14)$$

Because of limited power and sensitivity such measurements could not be made exactly with the system described here, but the results indicated ϵ_{db} to be less than -25 db for all of the five probes used.

A further check of the probe symmetry can be made by measuring the current distribution about a current minimum. On either side of a current null E_ρ is near a maximum and essentially constant in amplitude and phase, while B_θ changes by 180° in phase through the null. Any contributions to the probe current by E_ρ will add to those from B_θ on one side of the null and subtract on the other, producing an asymmetry in measurements through the null. The result of such a measurement is shown in Fig. 1-17. Points about the minimum are symmetrical within

the accuracy of measurement indicating low probe sensitivity to E_ρ. As pointed out by Whiteside, such asymmetry in the standing wave is caused only by the imaginary part of the error ratio. The real part of ϵ contributes nothing to such asymmetry.

Along that portion of the conductor which extends above the groundplane to form the antenna, the preceding remarks about E_ρ still hold. However, the situation in this region is complicated by the existence of E_z which is zero along the conductor but is not zero a short distance away where the probe gap is located and hence can maintain currents in the probe. Assuming the sensitivity to E_ρ to be negligible, the current in the probe is

$$I_L = S_B(vB_0) + S_E E_z = S_B(vB_0)\left[1 + \frac{S_E}{S_B}\frac{E_z}{vB_0}\right] = S_B(vB_0)\left[1 + \epsilon\frac{E_z}{vB_0}\right] \qquad (1.15)$$

ϵ as measured above is about 0.06. Consider a half wave dipole ($h = \lambda/4$) for which the fields are [17]

$$B_0 = \frac{jI_m\mu_o}{4\pi\rho}\left[e^{-j\beta r_{1h}} + e^{-j\beta r_{2h}}\right] \qquad (1.16)$$

$$E_z = \frac{-jI_m\zeta_o}{4\pi\rho}\left[\frac{e^{-j\beta r_{1h}}}{r_{1h}} + \frac{e^{-j\beta r_{2h}}}{r_{2h}}\right] \qquad (1.17)$$

$$E_\rho = \frac{jI_m\zeta_o}{4\pi\rho}\left[\frac{z-h}{r_{1h}}e^{-j\beta r_{1h}} + \frac{z+h}{r_{2h}}e^{-j\beta r_{2h}}\right] \qquad (1.18)$$

$r_{1h} = \sqrt{(h-z)^2+\rho^2}$, $r_{2h} = \sqrt{(h+z)^2+\rho^2}$; $\rho = \rho_o$ = probe radius = 0.00221 λ_o .

$$\frac{E_z}{vB_0} = \frac{-\rho_o}{r_{1h}} \left[1 + \frac{r_{1h}}{r_{2h}} e^{j\beta(r_{1h} - r_{2h})} \right] \frac{1}{\left[1 + e^{j\beta(r_{1h} - r_{2h})} \right]} \tag{1.19}$$

$$= \frac{-\rho_o}{r_{1h}} \left[\frac{1}{2+2\cos\beta(r_{1h}-r_{2h})} \right] \left[\left(\frac{r_{1h}}{r_{2h}}\right) + \left(\frac{r_{1h}}{r_{2h}} + 1\right)\cos\beta(r_{1h}-r_{2h}) + j\left(\frac{r_{1h}}{r_{2h}} - 1\right)\sin\beta(r_{1h}-r_{2h}) \right] \tag{1.20}$$

When the probe is located very near $z = 0$

$$\left| \frac{E_z}{vB_0} \right|_{z=0} = \frac{\rho_o}{r_{1h}} \doteq 8.84(10^{-3})$$

and the error term becomes

$$\left| \epsilon \frac{E_z}{vB_0} \right| = .005304$$

so that when the probe is located near the center of the antenna ($z/\lambda = 0$), currents in the probe maintained by E_z will be insignificant compared to those maintained by B_0. As the probe is moved toward the antenna end at $z = h$ the ratio $\frac{E_z}{vB_0}$ increases. Equation (1.20) gives the following values:

TABLE 1-5

ERROR IN PROBE CURRENT

z/λ	$\frac{E_z}{vB_0}$	$\left\lvert \frac{E_z}{vB_0} \right\rvert$	$\left\lvert \epsilon \frac{E_z}{vB_0} \right\rvert$
.20	-.0245 + j 0.0605	.0653	.003918
.21	-.0452 + j 0.1195	.1278	.007668
.22	-.0672 + j 0.1799	.1921	.011526
.24	-.0568 + j 0.5542	.5571	..033426

Thus, the small probe described in Section 1.2 will give an accurate indication of B_0 nearly to the antenna end at $z = h$. If the probe were much larger or much less symmetrical, its use to accurately measure B_0 would be restricted to $z/h \leq .85$. Although $\frac{E_z}{vB_0}$ has been calculated specifically for $h = \lambda/4$, the behaviour near $z = h$ will be similar for other values of h.

REFERENCES
(Chapter 1)

1. Morita, T., "The Measurement of Current and Charge Distributions on Cylindrical Antennas", Technical Report No. 66, Cruft Laboratory, Harvard University, Cambridge, Mass., February 1, 1949; also:

   Proc. I.R.E. 38, 898 (1950).

2. Moritz, C., "The Coupled Receiving Antenna, II", Technical Report No. 147, Cruft Laboratory, Harvard University, Cambridge, Mass., March, 1952.

3. Andrews, H. W., "Image-Plane and Coaxial Line Measuring Equipment at 600 Mc", Technical Report No. 177, Cruft Laboratory, Harvard University, Cambridge, Mass., July, 1953.

4. King, R. W. P., The Theory of Linear Antennas, Harvard University Press, Cambridge, Mass. (1956), pp. 193-237, 322-350.

5. King, R. W. P., "The End Correction for a Coaxial Line When Driving an Antenna over a Ground Screen", PGAP, AP-3, 66, 1955.

6. Ginzton, E. L., Microwave Measurements, McGraw-Hill Book Co., Inc., New York (1957), p. 269-275.

7. "Styrofoam HD-1, Styrofoam HD-2", Booklet 171-84, Plastics Dept., Dow Chemical Co., Midland, Michigan, September, 1957.

8. Handbook of Chemistry and Physics, Chemical Rubber Publishing Co., Cleveland, Ohio, 30th edition, (1948), p. 1953.

9. King, R. W. P., Transmission-Line Theory, McGraw-Hill Book Co., Inc., New York (1955), p. 95.

10. Montgomery, C. S., Techniques of Microwave Measurements, Rad. Lab. Series, 11, 480, McGraw-Hill Book Co., Inc., New York (1947).

11. Harris, E. F., "An Experimental Investigation of the Corner Reflector Antenna", Proc. I.R.E. 41, 685 (1953).

12. Whiteside, H., "Electromagnetic Field Probes", Technical Report No. 377, Cruft Laboratory, Harvard University, Cambridge, Mass., October, 1962.

13. King, R. W. P., Transmission-Line Theory, McGraw-Hill Book Co., Inc., New York (1955), p. 233.

14. Burton, R., "A Study of the Slot Transmission-Line and Slot Antenna, Part 2, A Coaxial Amplitude-Insensitive Phase-Detection System", Technical Report No. 398, Cruft Laboratory, Harvard University, Cambridge, Mass., January, 1963.

15. Ginzton, op. cit., p. 144.

16. Meier, A. S., and W. P. Summers, "Measured Impedances of Vertical Antennas Over Finite Groundplanes", Proc. I.R.E. 37, 609 (1949).

17. King, R. W. P., The Theory of Linear Antennas, Harvard University Press, Cambridge, Mass. (1956), p. 528.

18. Montgomery, C. S., op. cit., p. 486.

19. Tomiyasu, K., "Loading and Coupling Effects of Standing-Wave Detectors", Proc. I.R.E., 37, 1949.

20. King, R. W. P., Transmission-Line Theory, McGraw-Hill Book Co., Inc., New York (1955), pp. 22, 80.

21. King, R. W. P., "The Loop Antenna as a Probe in Arbitrary Electromagnetic Fields", Technical Report No. 262, Cruft Laboratory, Harvard University, Cambridge, Mass., May, 1957; also:

Handbuch der Physik, XVI, Springer-Verlag, Berlin, p. 270.

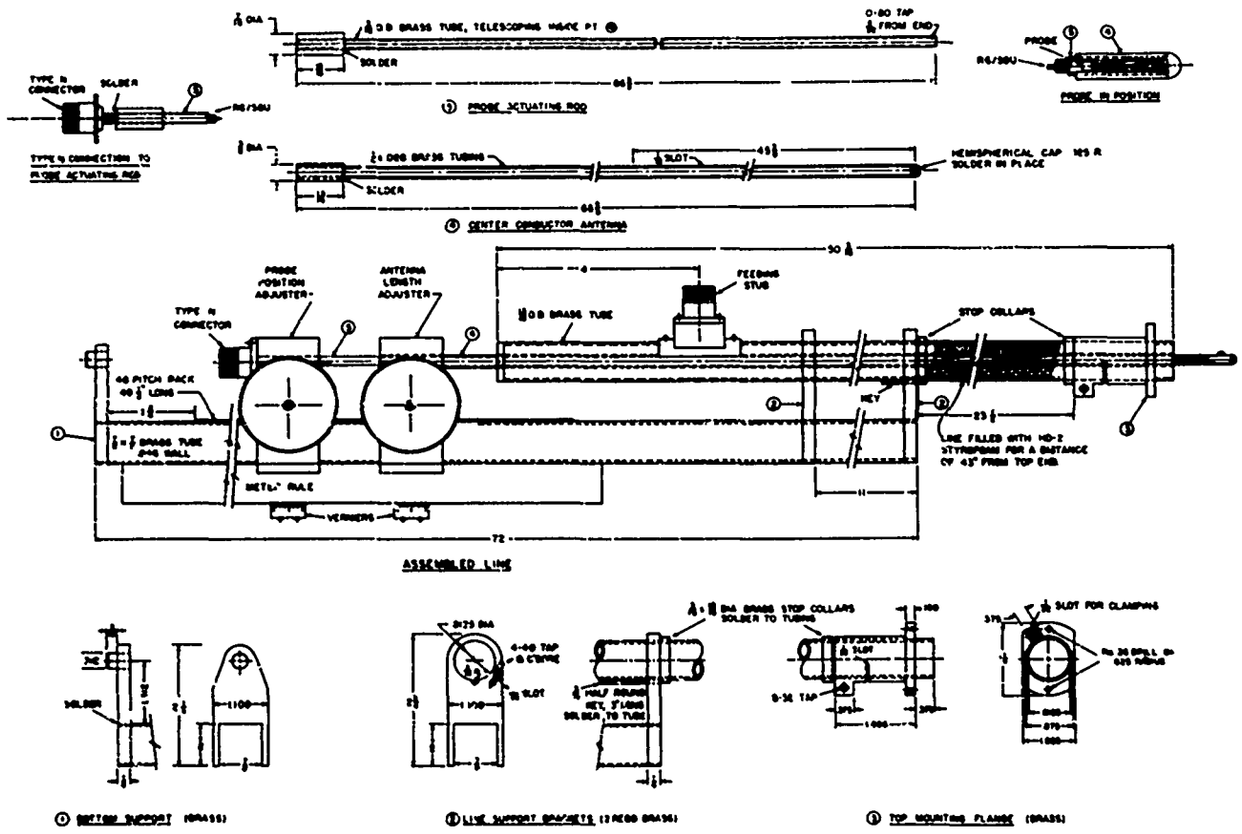

FIG 1-1 MEASURING LINE AND ANTENNAS

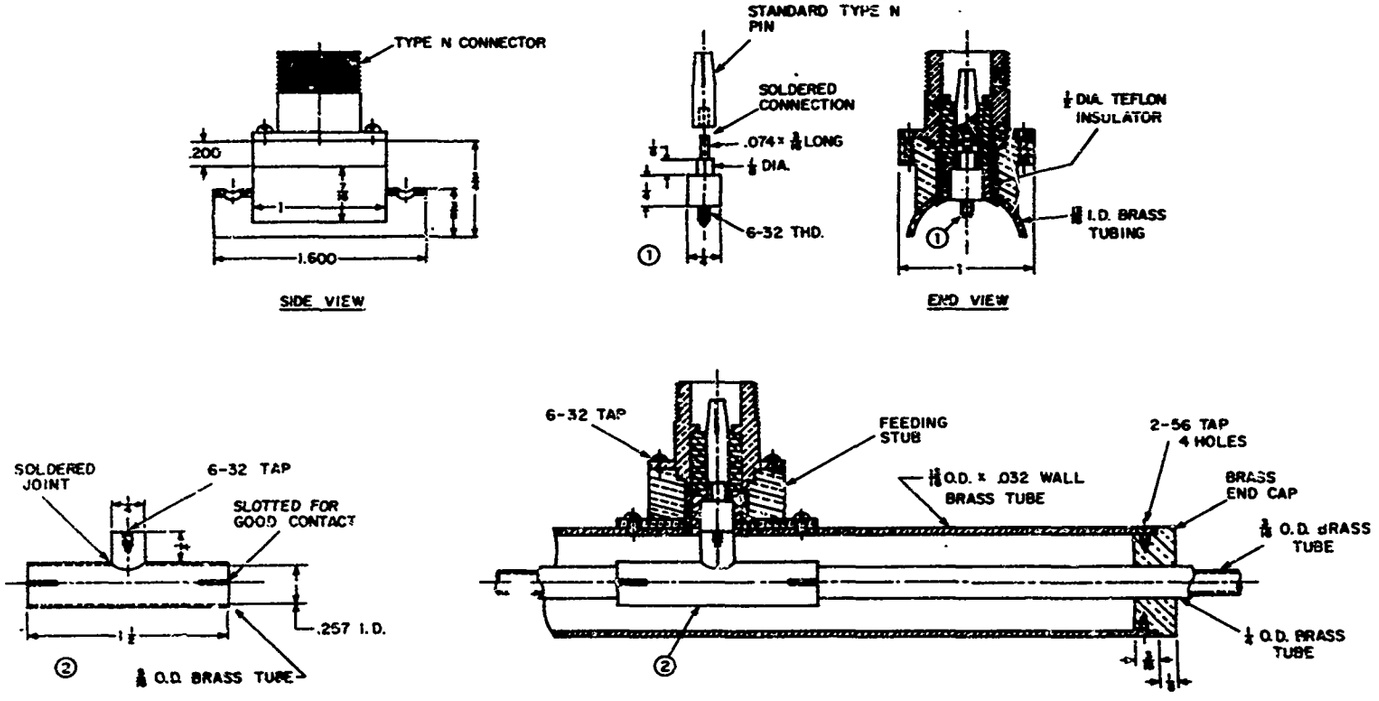

FIG. 1-2 FEEDING STUB DETAIL

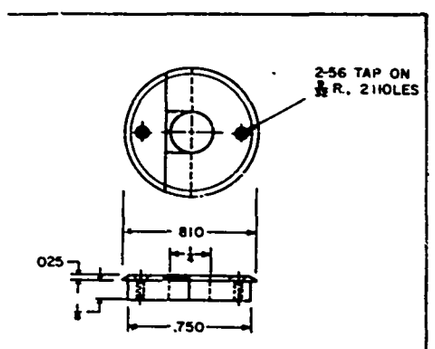

2 PIECE SHORT CIRCUIT

FIG. 1-4 SHORTING PLUG

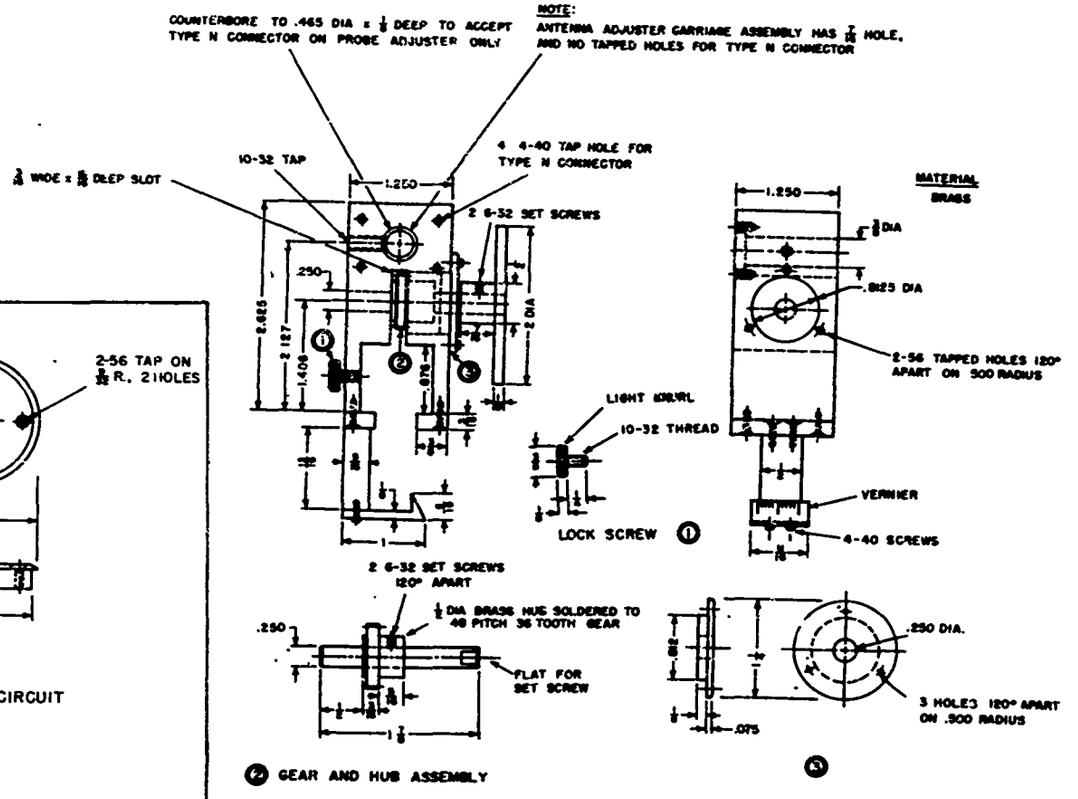

FIG. 1-3 ANTENNA AND PROBE ADJUSTER CARRIAGE

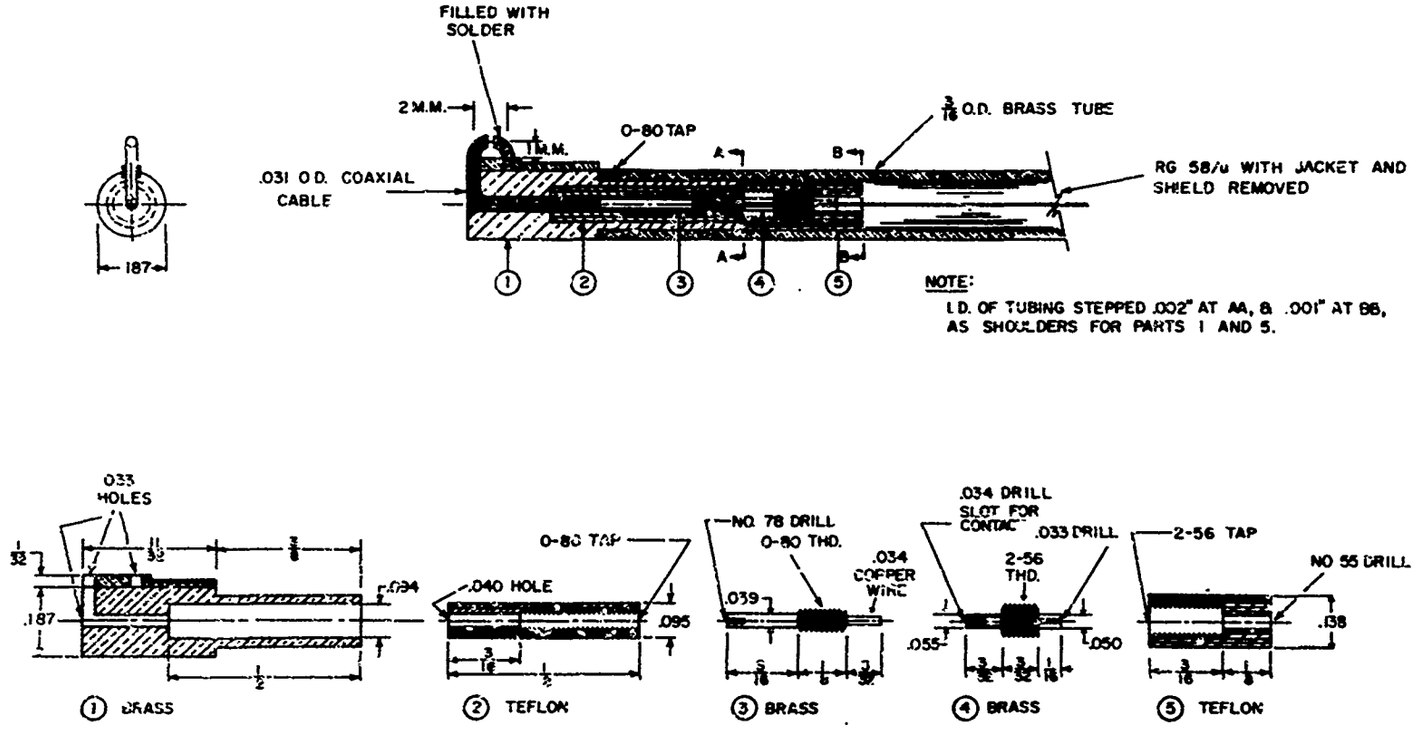

FIG. 1-5 BALANCED LOOP PROBE

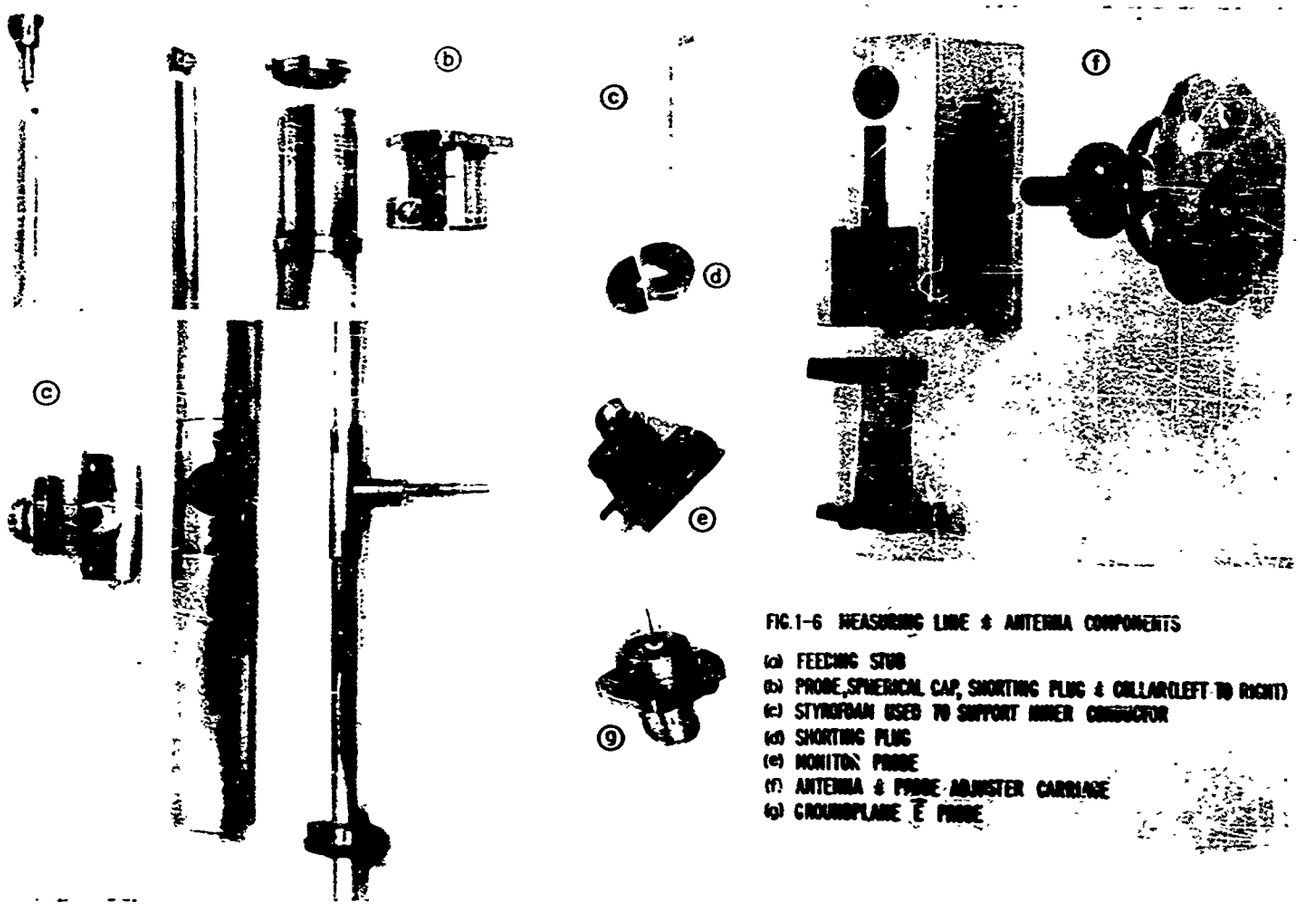

FIG.1-6 MEASURING LINE & ANTENNA COMPONENTS

(a) FEEDING STUB
(b) PROBE, SPHERICAL CAP, SHORTING PLUG & COLLAR(LEFT TO RIGHT)
(c) STYROFOAM USED TO SUPPORT INNER CONDUCTOR
(d) SHORTING PLUG
(e) MONITOR PROBE
(f) ANTENNA & PROBE ADJUSTER CARRIAGE
(g) GROUNDPLANE & PROBE

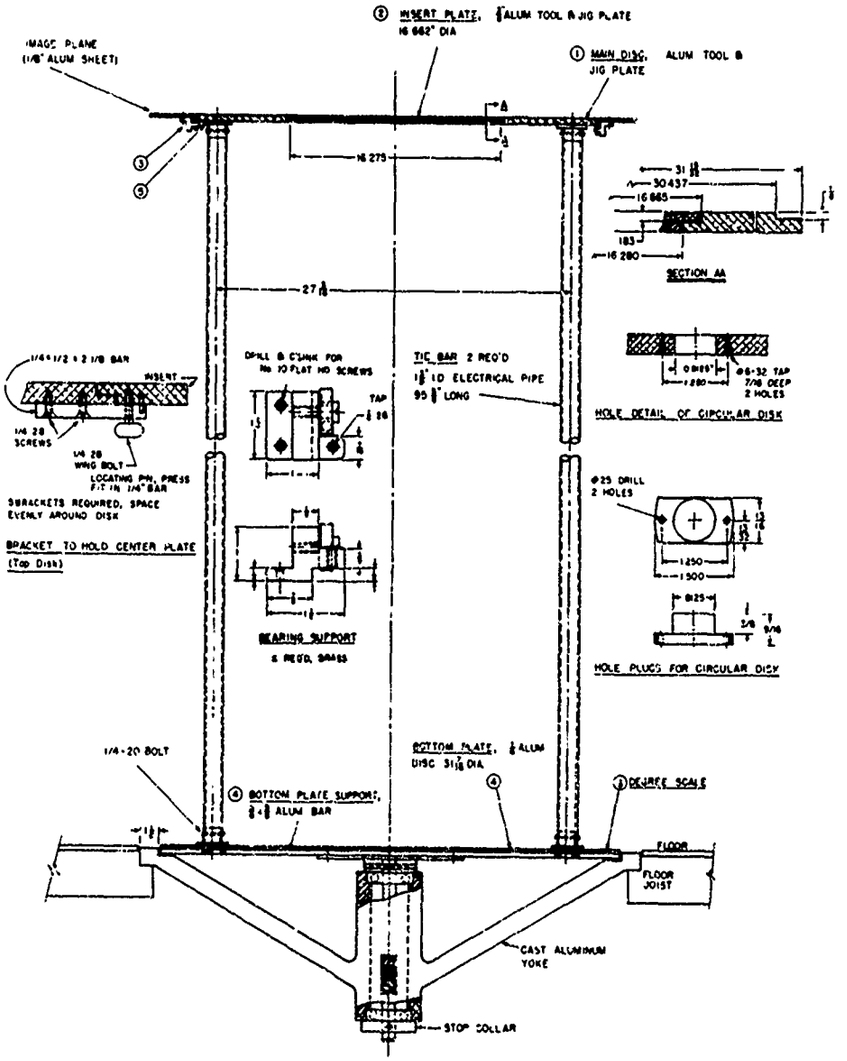

FIG 1-7 TURNTABLE MOUNT

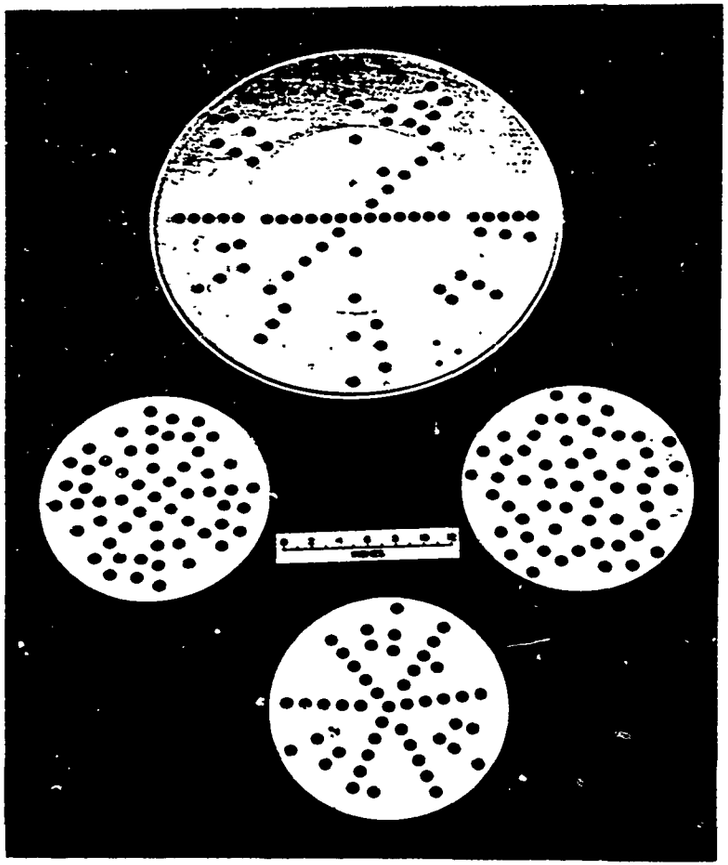

FIG 1-8a TOP CIRCULAR DISKS AND INSERTS

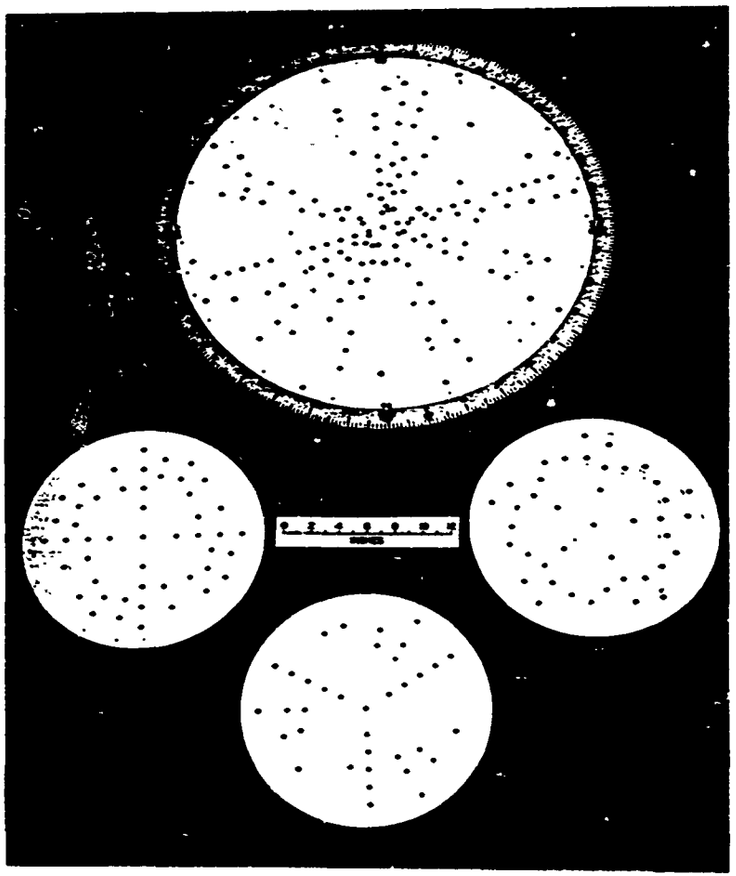

FIG. 1-8b BOTTOM PLATES

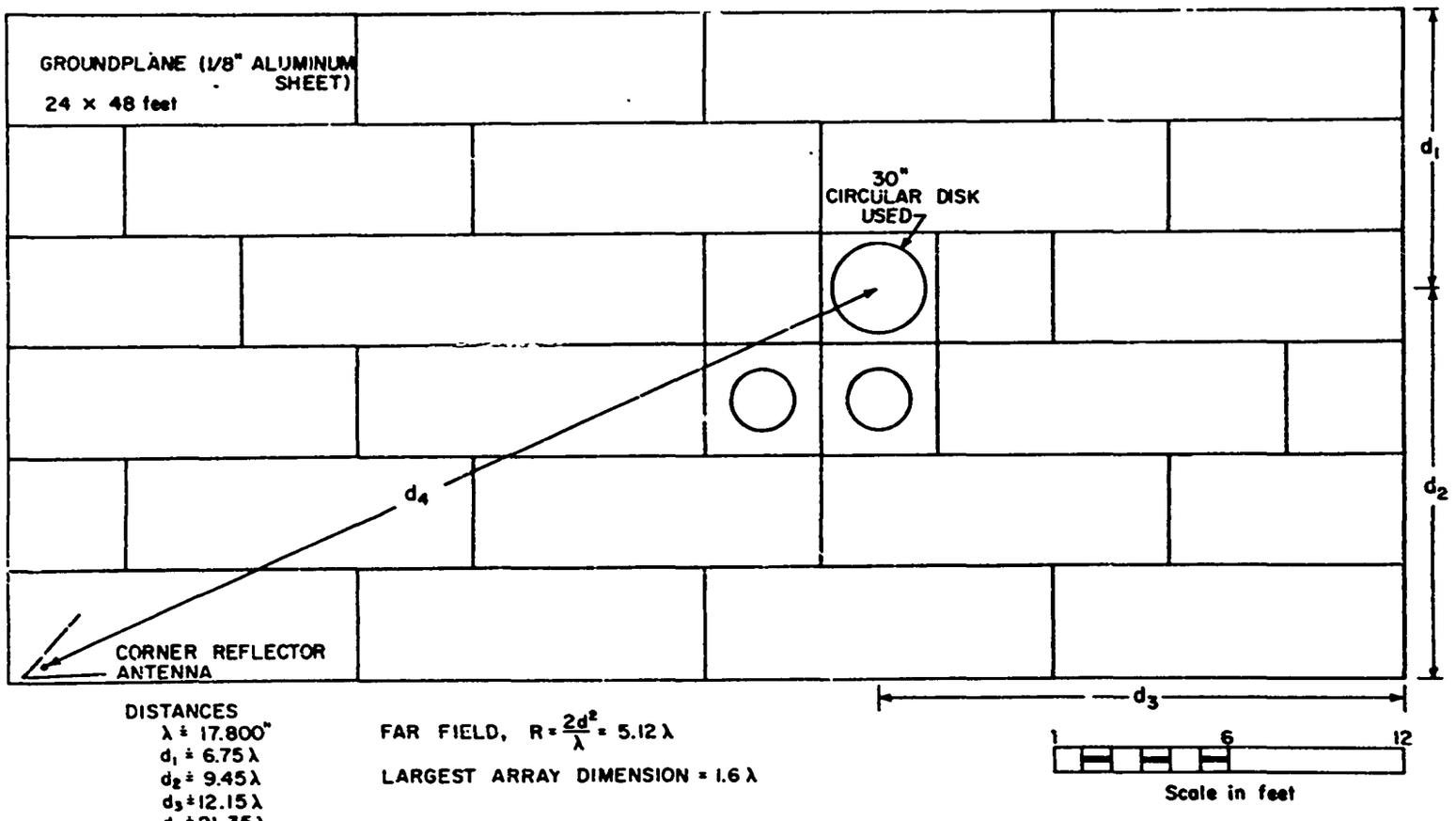

FIG. 1–9 GROUNDPLANE SURFACE

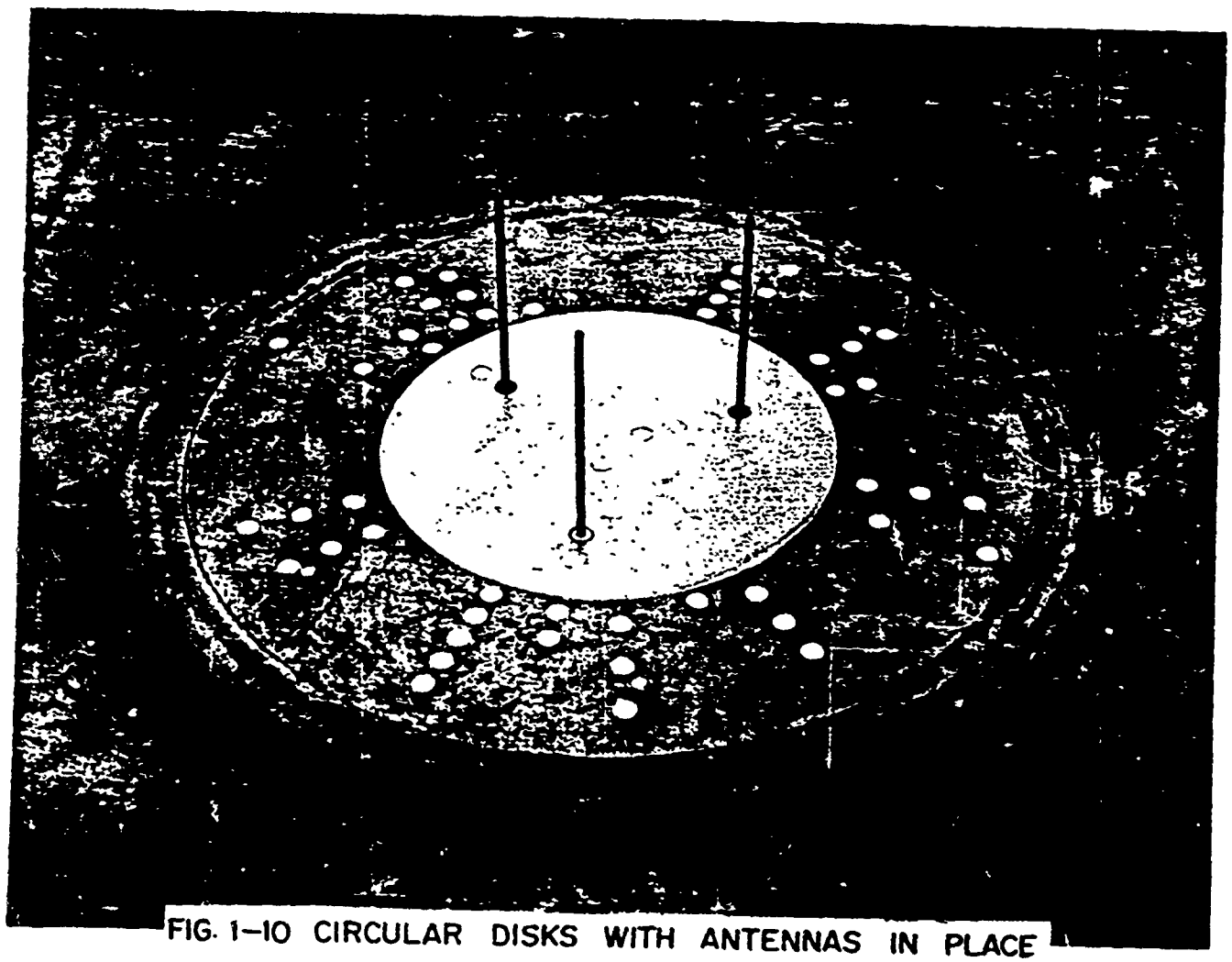

FIG. 1–10 CIRCULAR DISKS WITH ANTENNAS IN PLACE

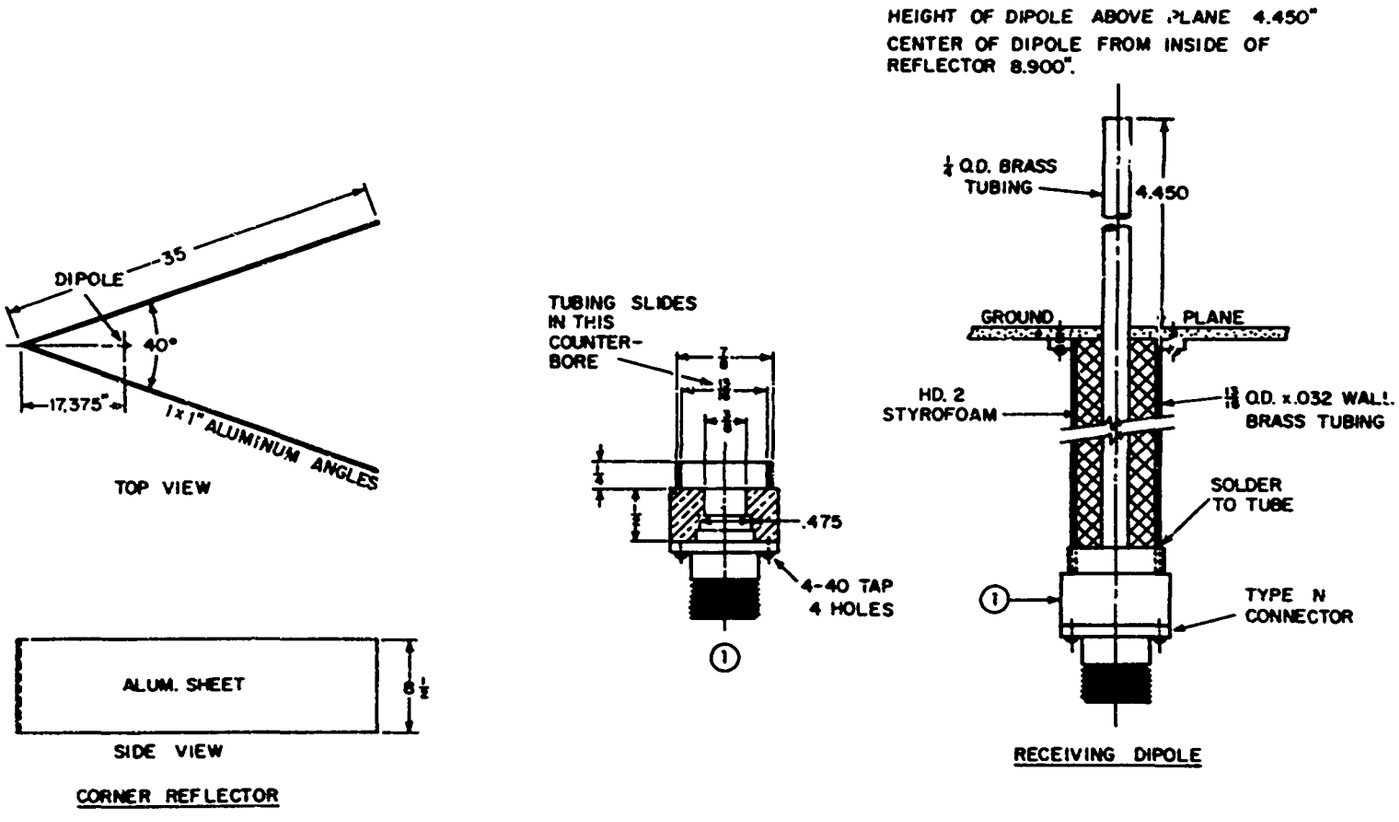

FIG. 1-11 CORNER REFLECTOR ANTENNA

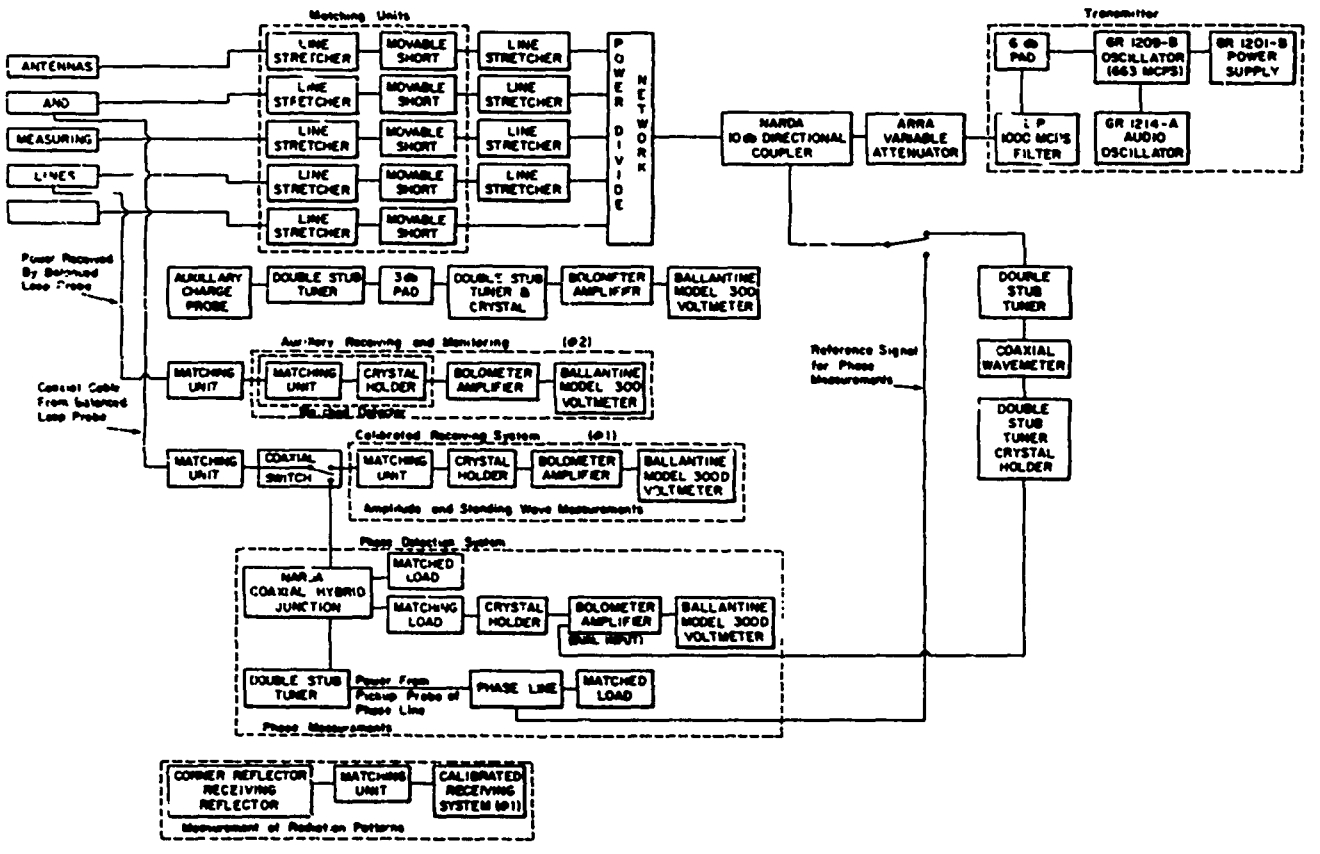

FIG. 1-12 RECEIVING AND TRANSMITTING EQUIPMENT

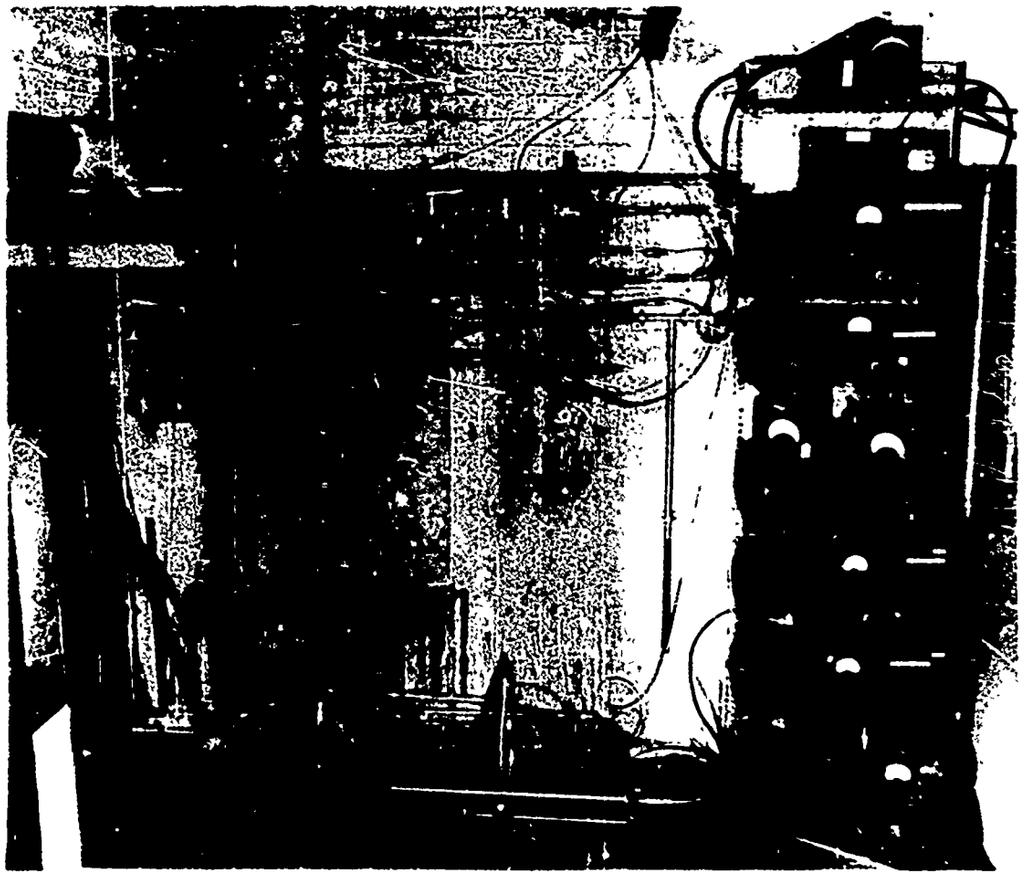

FIG. 1-13 EQUIPMENT MOUNTING ARRANGEMENT

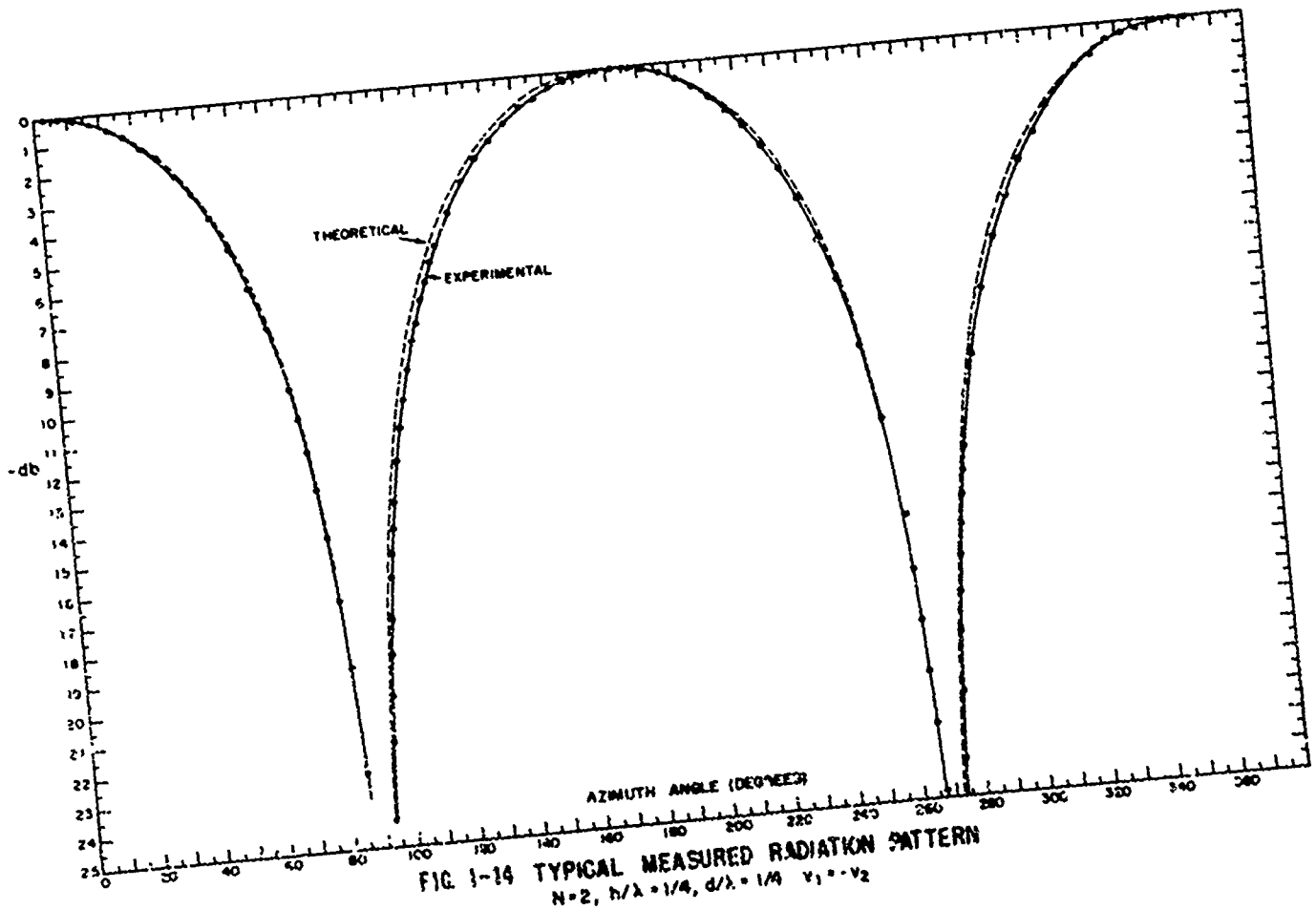

FIG. 1-14 TYPICAL MEASURED RADIATION PATTERN
N=2, $h/\lambda = 1/4$, $d/\lambda = 1/4$ $V_1 = -V_2$

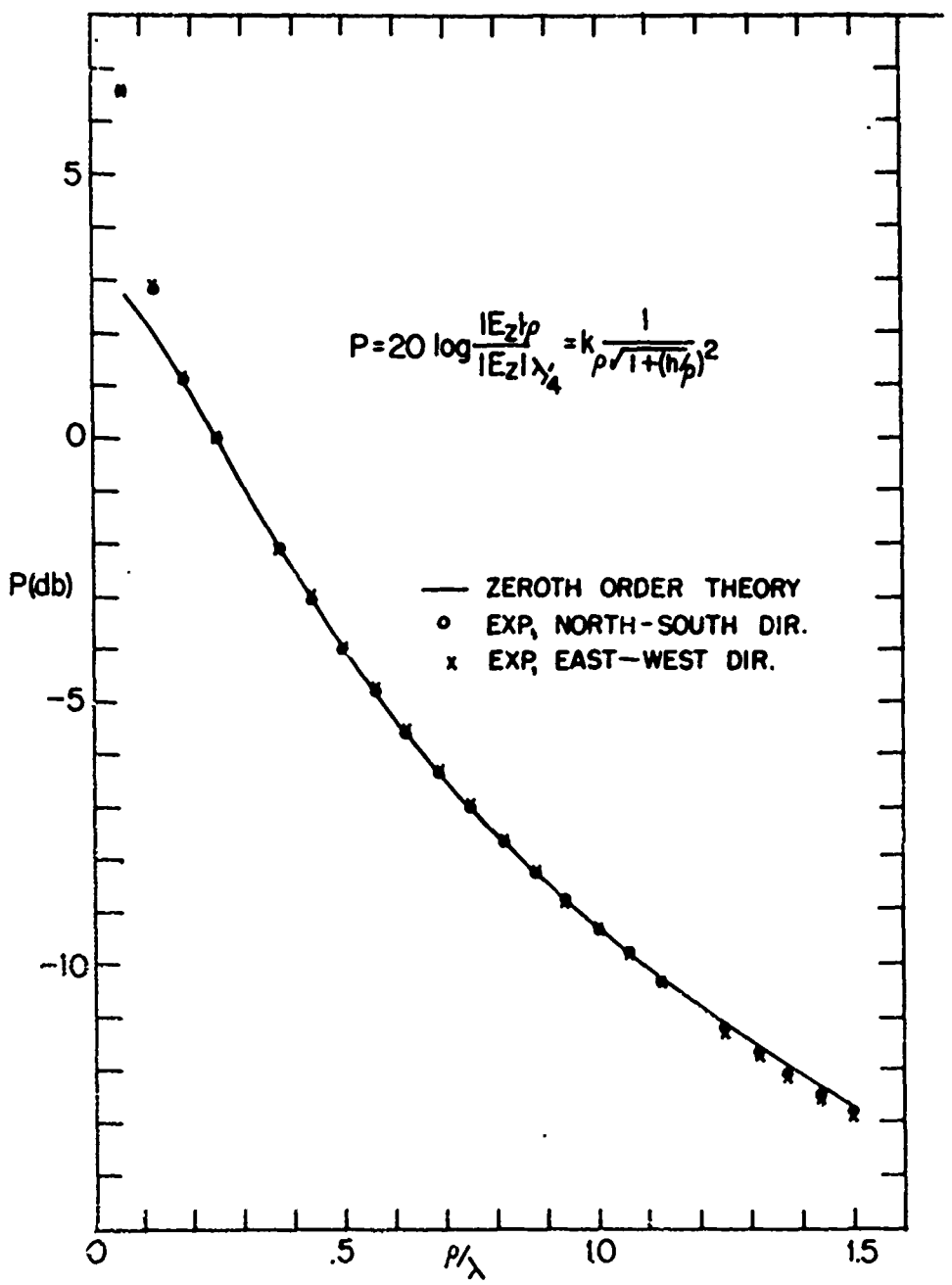

FIG. 1-15 VARIATION IN $|E_z|$ NEAR ANTENNA

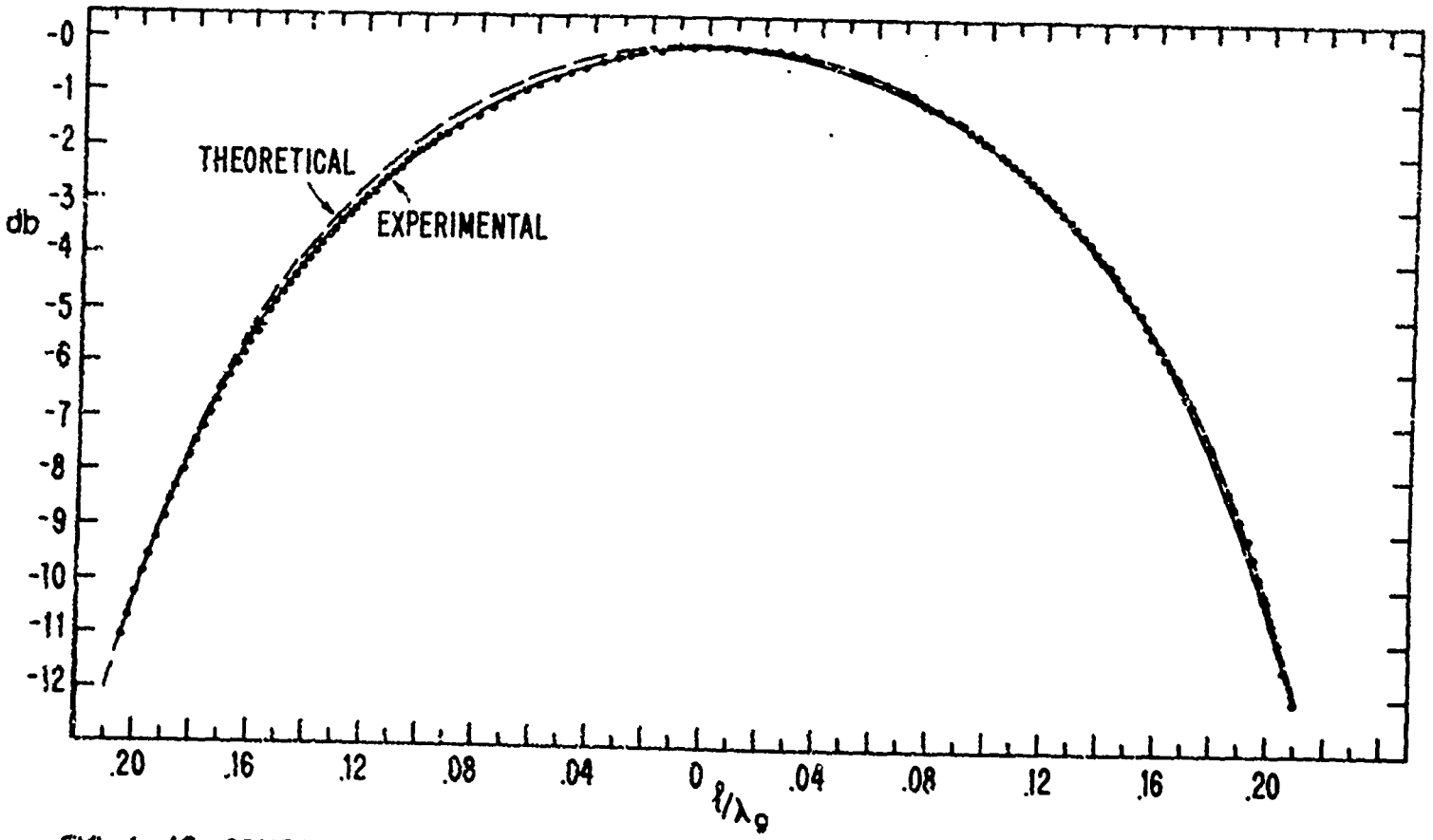

FIG. 3-16 COMPARISON OF MEASURED & THEORETICAL MAXIMA ON SHORTED LINE

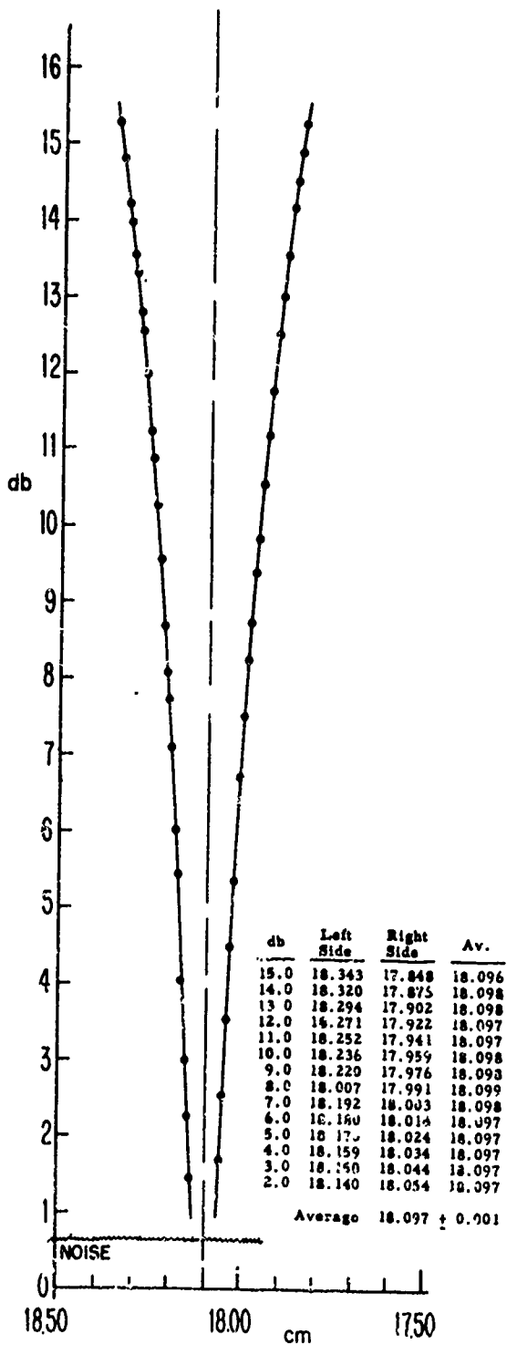

db	Left Side	Right Side	Av.
15.0	18.343	17.848	18.096
14.0	18.320	17.875	18.098
13.0	18.294	17.902	18.098
12.0	18.271	17.922	18.097
11.0	18.252	17.941	18.097
10.0	18.236	17.959	18.098
9.0	18.220	17.976	18.098
8.0	18.007	17.991	18.099
7.0	18.192	18.003	18.098
6.0	18.180	18.014	18.097
5.0	18.170	18.024	18.097
4.0	18.159	18.034	18.097
3.0	18.150	18.044	18.097
2.0	18.140	18.054	18.097
		Average	18.097 ± 0.001

FIG. 1-17 MINIMUM ON SHORTED LINE, SHOWING SYMMETRY